2011 50th IEEE Conference on Decision and Control and
European Control Conference (CDC-ECC)
Orlando, FL, USA, December 12-15, 2011

Parametric MIMO parallel Wiener identification

Maarten Schoukens and Yves Rolain

***Abstract*— This paper proposes a parametric identification method for multi-input multi-output parallel Wiener systems. The linear dynamic parts of the system are modeled by a parametric rational function in the continuous or discrete time variable, while the static nonlinearities are represented by a linear combination of nonlinear basis functions. The identification method uses a three step procedure to obtain initial estimates. In the first step, the frequency response matrix of the best linear approximation is estimated for different input excitation levels. In the second step, the power dependent dynamics are decomposed over a number of parallel orthogonal branches. In the last step, the static nonlinearities are estimated using a linear least squares estimation. Finally both linear and nonlinear parameters are estimated together using a nonlinear optimization procedure. The method is illustrated on a simulation example.**

I. Introduction

Wiener systems consist of a linear time invariant (LTI) dynamic system connected in tandem to a static nonlinearity. These systems are used to model nonlinear systems for which the nonlinearity can be concentrated mainly at the output, or when sensor nonlinearities are present [1]. This model suffers from a lack of general applicability. A generalization of the Wiener model to parallel Wiener models is presented in [2], [3], [4]. Such a parallel Wiener model consists of a parallel connection of Wiener systems and can cope with the presence of different signal paths from the input to the output. It is shown in [3] that parallel Wiener models can approximate any Volterra series of finite order.

This kind of model structure appears naturally for example in microwave power amplifiers. The main part of the signal is amplified to the output in a nonlinear way, through the signal path. Some distorted part of the signal can also find its way to the power supply terminal connection, and eventually appear at the output after reflection and frequency translation. Such systems can be better modeled by the parallel connection of Wiener systems. Furthermore, microwave power amplifiers are modeled as two-port devices. This requires the parallel Wiener identification method to be extended to multi-input multi-output (MIMO) parallel Wiener systems.

This paper proposes an identification method that extends the identification of parallel Wiener systems to MIMO parallel Wiener systems. Few identification methods for MIMO Wiener systems are described in the literature. Previous work on the identification of MIMO Wiener systems used for example a subspace approach [5], or an instrumental variables approach [6]. To the authors knowledge, none of

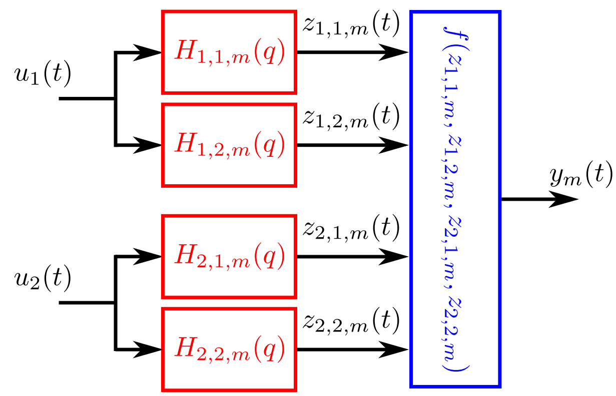

Fig. 1. 2-input, 1-output MISO parallel Wiener structure with 2 branches for each input. f-blocks: static nonlinearities, H-blocks: LTI.

these methods supports a parallel structure from the inputs to the outputs.

The main contributions of this paper are:

1) The expansion of parallel Wiener system identification to the MIMO case.
2) To obtain a parallel model whose number of branches is independent of the degree of nonlinearity. These branches have a physical interpretation.
3) To select the number of branches based on results of the identification method.
4) To model the LTI blocks using rational transfer functions.
5) To be applicable to both discrete- and continuous time models.

The first part of the paper describes the setup. Next the identification procedure is discussed in some detail, Finally an illustration on a simulation example shows the theoretical efficiency and the practical usefulness of the estimator.

II. Setup

This section introduces the considered class of systems, the class of excitation signals, and the noise disturbance model.

A. System and model

The class of nonlinear systems considered here is the class of MIMO parallel Wiener systems as is shown in Figure 1. For the sake of brevity, this paper only considers discrete time linear dynamic systems $H_{k,l,m}(q)$, with q^{-1} the backwards shift operator. The method works equally well for continuous time systems however. The static nonlinearity of each branch is modeled as a linear combination of

M. Schoukens is with Department ELEC, Vrije Universiteit Brussel, Belgium maarten.schoukens@vub.ac.be
Y. Rolain is with Department ELEC, Vrije Universiteit Brussel, Belgium yves.rolain@vub.ac.be

basis functions, for example it can be written in a power polynomial form.

$$z_{k,l,m}(t) = H_{k,l,m}(q)u_k(t) \tag{1}$$

$$\begin{aligned} y_m(t) &= f_m(z_{1,1,m}, \dots, z_{1,L,m}, z_{2,1,m}, \dots, z_{K,L,m}) \quad (2) \\ &= \sum_{i_{1,1}=0}^{d} \sum_{i_{1,2}=0}^{d-i_{1,1}} \cdots \sum_{i_{K,L}=0}^{d-i_{1,1}-\dots-i_{K,L-1}} \\ &\quad \alpha_m^{[i_{1,1},i_{1,2},\dots,i_{K,L}]} z_{1,1,m}^{i_{1,1}}(t) z_{1,2,m}^{i_{1,2}}(t) \dots z_{K,L,m}^{i_{K,L}}(t) \end{aligned}$$

herein d is the maximum degree of the nonlinearity, K the number of inputs, l is the running index indicating the corresponding parallel branch, with L the considered number of branches put in parallel for each input of the actual model, and m is the running index indicating the corresponding MISO (multi input single output) subsystem. $H_{k,l,m}(q)$ is the linear dynamic single-input-single-output (SISO) system that is associated to branch l and input k of MISO subsystem m.

B. Excitation signals

We will use excitation signals that belong to the extended class of Gaussian signals with fixed power spectrum $S_{U_0U_0}(f)$. Besides Gaussian noise this class includes also random phase multisine signals [7], [8], [9]. A periodic signal $u_0(t)$ with period length N is a member of a random phase multisine excitation set if:

$$\begin{aligned} u_0(t) &= N^{-1/2} \sum_{k=-N/2+1}^{N/2-1} U_k e^{j(2\pi k \frac{t}{N} + \varphi_k)} \quad k \neq 0 \\ &= N^{-1/2} \sum_{k=1}^{N/2-1} 2U_k cos(2\pi k \frac{t}{N} + \varphi_k), \end{aligned} \tag{3}$$

where $U_{-n} = U_n$ and $\varphi_{-n} = \varphi_n$. The phases φ_n are random variables that are independent over the frequency and have a (discrete) uniform distribution on the interval $[0, 2\pi[$, such that $E\{e^{j\varphi_n}\} = 0$. The amplitude U_n is set in a deterministic way by the user. Random phase multisines have the advantage of being periodic, which will cancel leakage effects. They offer also a full control over the applied amplitude spectrum to the user. When an infinite number of realizations is considered, a random phase multisine behaves as Gaussian noise.

C. Disturbing noise framework

An output error framework is assumed for the noise, and hence one noise source $v_m(t)$ for each output y_m is considered to be present at the output of the device under test (DUT):

$$y_m(t) = y_{m,0}(t) + v_m(t), \tag{4}$$

with $v_m(t)$ a random variable with an arbitrary power spectrum $S_{v_m v_m}(f)$. This noise source is assumed to generate additive colored (Gaussian) noise with finite second and fourth order moments. Finite fourth order moments are necessary to prove the asymptotic convergence properties of the estimator when the amount of data points grows to infinity [10].

III. Methodology

The proposed identification method is explained in this section. First a summary outline of the proposed method is given. Thereafter, the different subproblems are discussed in detail (estimating a best linear approximation (BLA) of the system, estimating the LTI-blocks and estimating the static nonlinearity).

A. Basic approach

The identification problem is divided in two subproblems, similar to what is described in [11] for parallel Hammerstein systems. First the linear dynamics of the different branches are estimated as follows:

1) A BLA of the complete system is estimated. This gives a linear approximation of the dynamics that are present in the system.
2) If excitation signals belonging to the Gaussian class of signals are used, Bussgang's theorem shows that the nonlinearity of each branch acts as a gain factor, depending on the total power [12], [7].
3) The BLA of a parallel Wiener system is a weighted sum of the LTI block response of each branch, where the static nonlinear block determines the unknown weighting factor for each branch.
4) If different excitation powers are used, different combinations of the same LTI blocks will be obtained.

This results in a set of equations that can be solved to find estimates for the LTI blocks of the parallel Wiener model.

Next, the static nonlinearities are estimated. To do so the output of the nonlinear basis functions, for example $(x_1^1, x_2^1, x_1^2, x_2^2, x_1^1 x_2^1, \dots, x_1^{d-1} x_2^1, x_1^1 x_2^{d-1}, x_1^d, x_2^d)$, are calculated. The corresponding coefficients of each basis function to each branch is estimated in least squares sense taking the intermediate outputs $y_{i,m}(t)$ as an input and $y_m(t)$ as the final output.

A parametric model is obtained by assembling all these sub-models in the parallel structure. This model will be used as the initial estimate to a Levenberg-Marquardt [13] optimization algorithm.

B. Estimating linear dynamics

The LTI blocks of the system will be estimated using a decomposition of the BLA of the complete system. First, a nonparametric method to estimate the BLA is explained. Second, a parametrization of this BLA is introduced. Finally, the decomposition of the parametrized BLA is performed.

1) MIMO Best linear approximation: The nonparametric BLA of the complete DUT is estimated for F different RMS (root mean square) values of the excitation signal to allow the separation of the dynamics of the different branches. The MIMO BLA is measured as a set of MISO systems, where all the signal paths in a particular MISO system leading to one output are computed simultaneously. To obtain the BLA from each input to each output, K experiments are made, generating K times all the input signals, where K is the number of inputs. The question how to design these different inputs is addressed in [9], where orthogonal multisines are introduced. Using these orthogonal multisines the MIMO BLA can be calculated using [14]:

$$\hat{\boldsymbol{G}}_m(j\omega_n) = \frac{1}{K} diag\left(|\boldsymbol{U}_K|^{-2}\right)\boldsymbol{Y}_m(j\omega_n)\boldsymbol{U}_K^H(j\omega_n) \quad (5)$$

where $|*|$ denotes the absolute value operator, and $diag(*)$ takes the diagonal of a square matrix. With $\boldsymbol{U}_K$ a matrix containing the orthogonal multisines of the different experiments and different input ports, $\boldsymbol{Y}_m$ a matrix containing the output signals m of the K different experiments:

$$\boldsymbol{U}_K(j\omega_n) = \begin{bmatrix} w_{11}U_1^{(1)}(j\omega_n) & w_{12}U_1^{(1)}(j\omega_n) & \cdots & w_{1K}U_1^{(1)}(j\omega_n) \\ w_{21}U_2^{(1)}(j\omega_n) & w_{22}U_2^{(1)}(j\omega_n) & \cdots & w_{2K}U_2^{(1)}(j\omega_n) \\ \vdots & \vdots & \ddots & \vdots \\ w_{K1}U_K^{(1)}(j\omega_n) & w_{K2}U_K^{(1)}(j\omega_n) & \cdots & w_{KK}U_K^{(1)}(j\omega_n) \end{bmatrix}$$

$$\boldsymbol{Y}_m(j\omega_k) = \begin{bmatrix} Y_m^{(1)}(j\omega_k) & Y_m^{(2)}(j\omega_k) & \cdots & Y_m^{(K)}(j\omega_k) \end{bmatrix} \quad (6)$$

where $U_K^{(i)}$ is the multisine input signal for the i-th experiment as defined in (3), and w_{ki} is a weighting factor for input k of experiment i. These weighting factors are entries of an arbitrary, deterministic, orthogonal matrix e.g. the discrete Fourier transform (DFT) matrix:

$$w_{ki} = e^{-j2\pi(k-1)(i-1)/K} \quad (7)$$

In practice, the BLA $\hat{G}_{k,m}$ from input k to output m is estimated with R different MIMO BLA experiments, using R different realizations of the random multisine. Each experiment encompasses P periods of the input. This allows one to access the frequency response matrix (FRM) of the BLA (describing the frequency response functions (FRF) from each input to each output), the power spectrum of the disturbing noise level, and the level of the nonlinear distortions separately [15]. For simplicity we assume here that the measurements start once the system transients are sufficiently damped (below the noise level). Note however that using improved FRF measurement methods, this waste of measurement time can be avoided [16]. Using equation (5) the BLA $\hat{G}_{k,m}^{[r,p]}(j\omega_n)$ for period p, and multisine realization r from input k to output m can be estimated. Each period p of each input signal realization r is used to obtain the FRF at a set of frequencies ω_n (9). The variability of the FRF that belongs to one realization yields the noise distortion variance $\hat{\sigma}^2_{\hat{G}_{k,m}^{[r]}}(n)$ (10), while the variability of the FRF over the different realizations yields the total distortion variance $\hat{\sigma}^2_{\hat{G}_{k,m}}(n)$ (11), including the nonlinear distortion of the DUT [15].

$$\hat{G}_{k,m}^{[r]}(j\omega_n) = \frac{1}{P}\sum_{p=1}^{P}\hat{G}_{k,m}^{[r,p]}(j\omega_n) \quad (8)$$

$$\hat{G}_{k,m}(j\omega_n) = \frac{1}{R}\sum_{r=1}^{R}\hat{G}_{k,m}^{[r]}(j\omega_n) \quad (9)$$

$$\hat{\sigma}^2_{\hat{G}_{k,m}^{[r]}}(j\omega_n) = \sum_{p=1}^{P}\frac{|\hat{G}_{k,m}^{[r,p]}(j\omega_k) - \hat{G}_{k,m}^{[r]}(j\omega_n)|^2}{P(P-1)} \quad (10)$$

$$\hat{\sigma}^2_{\hat{G}_{k,m}}(j\omega_n) = \sum_{r=1}^{R}\frac{|\hat{G}_{k,m}^{[r]}(j\omega_n) - \hat{G}_{k,m}(j\omega_n)|^2}{R(R-1)}, \quad (11)$$

This nonparametric FRF $\hat{G}_{k,m}(j\omega_n)$, and the total distortion variance $\hat{\sigma}^2_{\hat{G}_{k,m}}(j\omega_n)$ will be used in the next step to estimate a parametric model of the BLA of the DUT.

2) Transfer function parametrization : A downside of a nonparametric approach is the large amount of different realizations of the input signal that are necessary to average the disturbances towards zero. A parametric model of the BLA smooths the data also over the frequencies, and hence will reduce the variability of the estimates. This means that less input signal realizations will be required to achieve the same or a lower model variability.

The considered model is a rational function in z^{-1}:

$$\hat{G}_{BLA}(j\omega_k, \theta) = \frac{b_1 + b_2 z^{-1} + \cdots + b_{n_b+1}z^{-n_b}}{a_1 + a_2 z^{-1} + \cdots + a_{n_a+1}z^{-n_a}}, \quad (12)$$

with $n_b + n_a + 2$ parameters. Since one parameter can be chosen freely because of the scaling invariance of the transfer function, only $n_b + n_a + 1$ independent parameters need to be estimated. This leads to a significant reduction in the parameter count when compared with the nonparametric approach where N parameters must be estimated, with N the number of frequency lines.

A maximum likelihood estimator framework is used. As the estimator uses the previously estimated sample mean and sample variance of the BLA, a sample maximum likelihood estimator is used [17], [18]:

$$V_m(\theta_m, Z) = \sum_{n=1}^{N}\frac{|\hat{e}_m(j\omega_n, \theta_m, \hat{Z}(n))|^2}{\hat{\sigma}^2_{\hat{G}_{k,m}}(j\omega_n)}, \quad (13)$$

$$\hat{e}_m(j\omega_n, \theta_m, \hat{Z}(n)) = \hat{G}_{k,m}(j\omega_n) - \hat{G}_{k,m}(j\omega_n, \theta_m) \quad (14)$$

The parametrization for continuous time models is completely analog, using $s = j\omega$ instead of z^{-1}.

3) BLA decomposition: The F parametric transfer function models from one input to one output for all excitation levels of the input are evaluated on the same frequency grid as the nonparametric BLA estimate. The result is stored in a $N \times F$ matrix $\hat{\boldsymbol{G}}_{\boldsymbol{k,m}}$:

$$\hat{\boldsymbol{G}}_{\boldsymbol{k,m}} = \begin{bmatrix} \hat{G}_{k,m}^{[1]}(j\omega_1, \hat{\theta}_1) & \hat{G}_{k,m}^{[2]}(j\omega_1, \hat{\theta}_2) & \cdots & \hat{G}_{k,m}^{[F]}(j\omega_1, \hat{\theta}_F) \\ \hat{G}_{k,m}^{[1]}(j\omega_2, \hat{\theta}_1) & \hat{G}_{k,m}^{[2]}(j\omega_2, \hat{\theta}_2) & \cdots & \hat{G}_{k,m}^{[F]}(j\omega_2, \hat{\theta}_F) \\ \vdots & \vdots & \ddots & \vdots \\ \hat{G}_{k,m}^{[1]}(j\omega_N, \hat{\theta}_1) & \hat{G}_{k,m}^{[2]}(j\omega_N, \hat{\theta}_2) & \cdots & \hat{G}_{k,m}^{[F]}(j\omega_N, \hat{\theta}_F) \end{bmatrix}$$

This matrix is decomposed as explained in Section III-A, using a singular value decomposition (SVD). This gives three matrices as a result:

$$\hat{\boldsymbol{G}}_{\boldsymbol{k,m}} = U_{k,m}\Sigma_{k,m}V_{k,m}^T, \quad (15)$$

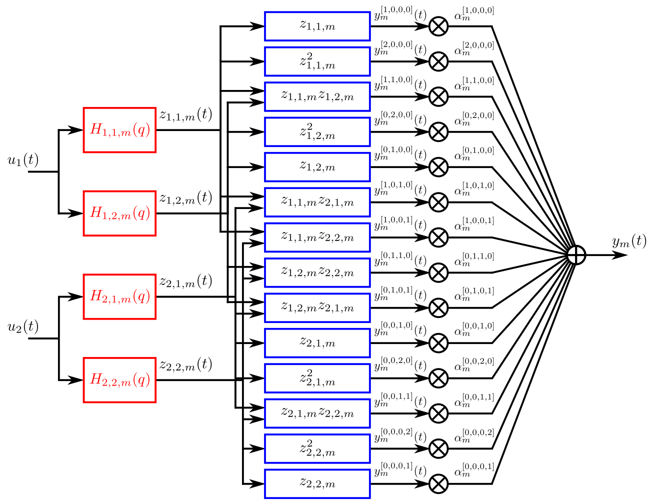

Fig. 2. MISO Parallel Wiener block diagram representing the static nonlinearity estimation of second degree for 2 branches and 2 inputs.

where the columns of $U_{k,m}$ contain the desired estimates of the LTI blocks:

$$U_{k,m} = \begin{bmatrix} \hat{H}_{k,1,m}(j\omega_1) & \hat{H}_{k,2,m}(j\omega_1) & \cdots & \hat{H}_{k,F,m}(j\omega_1) \\ \hat{H}_{k,1,m}(j\omega_2) & \hat{H}_{k,2,m}(j\omega_2) & \cdots & \hat{H}_{k,F,m}(j\omega_2) \\ \vdots & \vdots & \ddots & \vdots \\ \hat{H}_{k,1,m}(j\omega_N) & \hat{H}_{k,2,m}(j\omega_N) & \cdots & \hat{H}_{k,F,m}(j\omega_N) \end{bmatrix}$$

The columns of the $U_{k,m}$ matrix can be seen as a set of vectors that form an orthogonal basis for the space spanned by the $\hat{\boldsymbol{G}}_{\boldsymbol{k,m}}$ matrix. The magnitude of the singular values represent the importance of each basis vector, and the error that is made by neglecting them. This means that $\hat{\boldsymbol{G}}_{\boldsymbol{k,m}}$ can be approximated using a limited number of U columns. The error of this approximation depends on the singular values in the Σ matrix.

Hence, the first L columns of the U matrix, corresponding with the L highest singular values in the Σ matrix, give an estimate of the L different LTI blocks in the model. Even more, based on those singular values one can decide how many branches are needed to achieve a certain model quality. Indeed, the singular value $\sigma_{k,l}$ represents the importance of the corresponding LTI estimate $\hat{H}_{k,l,m}$ in the final model.

The obtained $\hat{H}_{k,l,m}(j\omega)$ estimate is nonparametric again, but it can be modeled by a rational form using the techniques described in Section III-B.2, resulting in the estimate $\hat{H}_{k,l,m}(j\omega, \theta_{k,l,m})$.

C. Estimating static nonlinearity

To estimate the static nonlinearities of the branches that compose the system, a known set of input signals $u_1(t), \ldots, u_K(t)$ with the corresponding set of outputs $y_1(t), \ldots, y_M(t)$ is selected. Define the outputs $y^{[i_{1,1}, i_{1,2}, \ldots, i_{1,L}, i_{2,1}, \ldots, i_{K,L}]}(t)$ of the nonlinear basis functions up to degree d (Figure 2), e.g.

$$z_{k,l,m}(t) = H_{k,l,m}(q)u_k(t) \tag{16}$$

$$y_m^{[i_{1,1}, i_{1,2}, \ldots, i_{1,L}, i_{2,1}, \ldots, i_{K,L}]}(t) = \prod_{l=1}^{L} \prod_{k=1}^{K} z_{k,l,m}^{i_{k,l}}(t), \tag{17}$$

$$1 \leq \sum_k \sum_l i_{k,l} \leq d$$

The modeled output of the parallel Wiener system will be a linear combination of these reference output signals:

$$\begin{aligned} y_m(t) &= B\theta_m \\ &= \sum_{i_{1,1}=0}^{d} \cdots \sum_{i_{K,L}=0}^{d-i_{1,1}-\ldots-i_{K,L-1}} \\ &\quad \alpha_m^{[i_{1,1}, \ldots, i_{K,L}]} y_m^{[i_{1,1}, \ldots, i_{K,L}]}(t), \end{aligned} \tag{18}$$

where B depends on the calculated outputs $y_{l,m}^{[i]}(t)$, and

$$\hat{\theta}_m = \begin{bmatrix} \hat{\alpha}_m^{[1,0,\ldots,0]} & \hat{\alpha}_m^{[0,1,\ldots,0]} & \ldots & \hat{\alpha}_m^{[0,0,\ldots,d]} \end{bmatrix} \tag{19}$$

The coefficients θ_m are estimated by solving the following over determined set of equations in least squares sense:

$$y_m = B\theta_m + v \tag{20}$$

which gives:

$$\hat{\theta}_m = (B^T B)^{-1} B^T y_m \tag{21}$$

This equation is solved using the pseudo-inverse of B [19]. The columns of B are normalized, dividing them by their 2-norm, to improve the numerical conditioning of the problem.

D. Estimated system

Once the static nonlinearity and the linear dynamics of each branch of each subsystem are known, it is possible to synthesize the full model that yields the outputs $y_m(t)$ of the total system for a set of input signals $u_1(t), u_2(t), \ldots, u_K(t)$. Based on the notations shown in Figure 1, one obtains:

$$\hat{z}_{k,l,m}(t) = \hat{H}_{k,l,m}(q)u_k(t)$$

$$\begin{aligned} \hat{y}_m(t) &= \sum_{i_{1,1}=0}^{d} \sum_{i_{1,2}=0}^{d-i_{1,1}} \cdots \sum_{i_{K,L}=0}^{d-i_{1,1}-\ldots-i_{K,L-1}} \\ &\quad \hat{\alpha}_m^{[i_{1,1}, i_{1,2}, \ldots, i_{K,L}]} \hat{z}_{1,1,m}^{i_{1,1}}(t) \hat{z}_{1,2,m}^{i_{1,2}}(t) \ldots \hat{z}_{K,L,m}^{i_{K,L}}(t) \end{aligned} \tag{22}$$

Because the identification procedure uses a decomposition of the BLAs of the system, a physical interpretation can even be given for this model. The detected number of branches can represent the number of independent signal flows that are present within the modeled system, and the singular value corresponding to a branch of the model represents the importance of the contribution of that branch in the model output.

E. Levenberg-Marquardt optimization

The estimates of Section III-D can be used as the initial estimates of a nonlinear iterative optimization algorithm to obtain more accurate model estimates. To do so a Levenberg-Marquardt optimization algorithm is implemented [13], [7]. This algorithm simultaneously optimizes the parameters of the static nonlinear blocks and LTI blocks present in the model.

The Levenberg-Marquardt optimization method is a local nonlinear optimizer. Hence, the obtained minimum of the cost function can be a local minimum. There is no guarantee that the global minimum is reached using the method proposed above.

IV. Simulation Example

A simulation experiment is performed and the simulation results are discussed.

A. Simulation setup

The procedure is illustrated on the simulation of a 2-input 1-output MISO 2-branch parallel Wiener system as shown in Figure 1 with additive disturbing output noise. The static nonlinear blocks are of the polynomial form and are of third degree. Crossterms are included in the static nonlinearities.

$$\begin{aligned} y_1(t) &= \alpha^{[1,0,0,0]} z_{1,1}(t) + \alpha^{[2,0,0,0]} z_{1,1}^2(t) + \alpha^{[3,0,0,0]} z_{1,1}^3(t) \\ &+ \alpha^{[0,1,0,0]} z_{1,2}(t) + \alpha^{[0,2,0,0]} z_{1,2}^2(t) + \alpha^{[0,3,0,0]} z_{1,2}^3(t) \\ &+ \alpha^{[0,0,1,0]} z_{2,1}(t) + \alpha^{[0,0,2,0]} z_{2,1}^2(t) + \alpha^{[0,0,3,0]} z_{2,1}^3(t) \\ &+ \alpha^{[0,0,0,1]} z_{2,2}(t) + \alpha^{[0,0,0,2]} z_{2,2}^2(t) + \alpha^{[0,0,0,3]} z_{2,2}^3(t) \\ &+ \alpha^{[1,1,0,0]} z_{1,1}(t) z_{1,2}(t) + \alpha^{[0,1,0,1]} z_{1,2}(t) z_{2,2}(t) \\ &+ \alpha^{[1,0,1,1]} z_{1,1}(t) z_{2,1}(t) z_{2,2}(t) \end{aligned} \tag{23}$$

The coefficients of the static nonlinearity are tuned so that for the selected amplitude range of the excitation (between 0.5 and 3 a.u.$_{rms}$ (arbitrary units)) both the even and the odd nonlinearities contribute significantly to the output (ranging from 60 to 20 dB lower than the output spectrum). The linear dynamics of each branch are chosen to be low-pass filters whose transfer function are given below:

$$H_{1,1}(z) = \frac{0.6860 + 2.0579z^{-1} + 2.0579z^{-2} + 0.6860z^{-3}}{1 - 2.2805z^{-1} + 1.7661z^{-2} - 0.4412z^{-3}} \tag{24}$$

$$H_{1,2}(z) = \frac{0.0017 + 0.0050z^{-1} + 0.0050z^{-2} + 0.0017z^{-3}}{1 - 2.6748z^{-1} + 2.5171z^{-2} - 0.8290z^{-3}} \tag{25}$$

$$H_{2,1}(z) = \frac{0.0071 + 0.0212z^{-1} + 0.0212z^{-2} + 0.0071z^{-3}}{1 - 2.2746z^{-1} + 1.8872z^{-2} - 0.5559z^{-3}} \tag{26}$$

$$H_{2,2}(z) = \frac{0.0035 + 0.0106z^{-1} + 0.0106z^{-2} + 0.0035z^{-3}}{1 - 2.4053z^{-1} + 2.0128z^{-2} - 0.5792z^{-3}} \tag{27}$$

The disturbance noise $v(t)$ is white Gaussian noise with a standard deviation of 10^{-5} $a.u.$, which gives a signal-to-noise ratio (SNR) between -90 and -120 dB depending on the input excitation level. The BLA is calculated over 2 periods for 20 realizations of the input over 10 RMS values, linearly distributed between 0.5 and 3 a.u.$_{rms}$. A random phase multisine with a constant power spectrum is used as an excitation. Excitations with a period length of 1024 data points are used and 127 frequencies are excited between DC and $0.124 f_{sample}$, with DC excluded. The sample frequency f_{sample} is normalized to one.

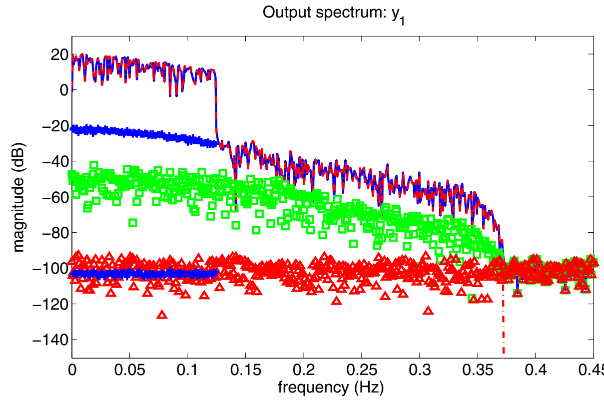

Fig. 3. Simulation output spectrum with noise on the output, signal to distortion ratio ≈ 40 (SDR) dB. Full line: output of the true system. Dash dotted line: output of the optimized model. Triangles: error of the optimized model, squares: initial estimated model. Top crosses: total variance within the excited frequency band, bottom crosses: noise variance within the excited frequency band.

B. Simulation results

The estimated nonlinear MISO parallel Wiener model before and after optimization are compared with the exact output of the simulated system in the presence of output noise, as is shown in Figure 3. The level of the total distortion and the additive noise distortion are calculated with the BLA-method, and are represented on the same graph.

The model resulting from the initial parameter estimates explains a significant part in the nonlinearities present of the system. The model error before optimization is already 20 to 40 dB lower then the total distortion present in the outputs of the simulated system. After optimization with the Levenberg-Marquardt optimization algorithm, the error further decreases down to the noise floor. This shows that the proposed identification method followed by a Levenberg-Marquardt optimization are able to model MISO, and with extension MIMO, parallel Wiener systems.

V. Conclusion

A parametric identification for MIMO parallel Wiener systems, using a three step procedure is presented, together with a Levenberg-Marquardt optimizer to further improve the estimates.

The idea is to first identify the best linear approximation (BLA) of the system for different excitation levels using either Gaussian noise or random phase multisine excitations. Next the dynamics of the individual branches are obtained by the decomposition of the BLAs. Finally, a linear least squares estimation of the nonlinearities for each branch of the system is made.

Compared with the existing algorithms for MIMO Wiener systems, a major advantage of this method is the possibility of modeling parallel branches, where the number of branches does not depend on the nature of the nonlinearities, but rather on the number of physical signal paths that are present in the system. This number of branches can be selected based on results of the identification method.

Acknowledgment: this work is sponsored by the Fund for Scientific Research (FWO-Vlaanderen), the Flemish Government (Methusalem), and the Belgian Federal Government (IUAP VI/4).

REFERENCES

[1] F. Giri and E.W. Bai. *Block-oriented Nonlinear System Identification*. Springer, 1 edition, 2010.

[2] M. Schetzen. *The Volterra and Wiener Theories of Nonlinear Systems*. Wiley, New York, 1980.

[3] S Boyd and LO Chua. Fading Memory and the Problem of Approximating Nonlinear Operators with Volterra Series. *IEEE Trans. Circuits Syst.*, 32(11):1150–1161, 1985.

[4] HC Ku, MD McKinley, and JS Kenney. Quantifying memory effects in RF power amplifiers. *IEEE Trans. Microw. Theory Tech.*, 50(12):2843–2849, DEC 2002.

[5] D Westwick and M Verhaegen. Identifying MIMO Wiener systems using subspace model identification methods. *Signal Processing*, 52(2):235–258, JUL 1996.

[6] A. Janczak. Instrumental variables approach to identification of a class of MIMO Wiener systems. *Nonlinear Dynamics*, 48(3):275–284, MAY 2007.

[7] R. Pintelon and J. Schoukens. *System Identification. A Frequency Domain Approach*. IEEE-press, Piscataway, 2001.

[8] J. Schoukens, J. Lataire, R. Pintelon, and G. Vandersteen. Robustness Issues of the equivalent linear representation of a nonlinear system. *IEEE Trans. Instrum. Meas.*, 58(5):1737–1745, 2009.

[9] T. Dobrowiecki, J. Schoukens, and P. Guillaume. Optimized excitation signals for MIMO frequency response function measurements. *IEEE Trans. Instrum. Meas.*, 55(6):2072–2079, 2006.

[10] J. Schoukens, T. Dobrowiecki, and R. Pintelon. Parametric and non-parametric identification of linear systems in the presence of nonlinear distortions. A frequency domain approach. *IEEE Trans. Autom. Contr.*, 43(2):176–190, 1998.

[11] M. Schoukens, Y. Rolain, R. Pintelon, and J. Schoukens. Semi-parametric identification of parallel Hammerstein systems. In *UKACC International Conference on CONTROL 2010*, Coventry University, UK, Sept 07-10 2010.

[12] J.J. Bussgang. Cross-correlation functions of amplitude-distorted Gaussian signals. Technical Report 216, MIT Laboratory of Electronics, 1952.

[13] R. Fletcher. *Practical Methods of Optimization*. Wiley & Sons, second edition, 1991.

[14] Tadeusz Dobrowiecki and Johan Schoukens. Measuring a linear approximation to weakly nonlinear MIMO systems. *Automatica*, 43(10):1737–1751, 2007.

[15] T. D'haene, R. Pintelon, J. Schoukens, and E. Van Gheem. Variance analysis of frequency response function measurements using periodic excitations. *IEEE Trans. Instrum. Meas.*, 54(4):1452–1456, 2005.

[16] R. Pintelon, J. Schoukens, G. Vandersteen, and K. Barbé. Estimation of nonparametric noise and FRF models for multivariable systems–Part I: Theory. *Mechanical Systems and Signal Processing*, 24(3):573–595, 2010.

[17] J. Schoukens, R. Pintelon, G. Vandersteen, and P. Guillaume. Frequency-domain system identification using non-parametric noise models estimated from a small number of data sets. *Automatica*, 33(6):1073 – 1086, 1997.

[18] T. Söderström, M. Hong, J. Schoukens, and R. Pintelon. Accuracy analysis of time domain maximum likelihood method and sample maximum likelihood method for errors-in-variables and output error identification. *Automatica*, 46(4):721 – 727, 2010.

[19] A. Ben-Israel and T.N.E. Greville. *Generalized Inverses: Theory and Applications*. Wiley-Interscience, second edition, 1974.